Opposit Page:

Photographs of a micro electric induction motor used in a motor compressor: (A) a wide view of the stator; (B) a close up view of the stator showing the outer edge of the stator electrodes and their connections to one phase lead; (C) a close up view of the stator electrodes showing the interconnection of electrodes of the same phase through buried interconnect rings; (D) the front side of the rotor showing the compressor blades, and the back side of the rotor showing the rotor conductor.
Photo Courtesy of C. Livermore, S. D. Umans, E. P. Warren and X. Zhang
(J. H. lang, A. H. Epstein, M. A. Schmidt and S. D. Senturia, and A. Forte of MIT Lincoln Lab)
Research sponsored by ARO and DARPA.

Microelectromechanical Devices

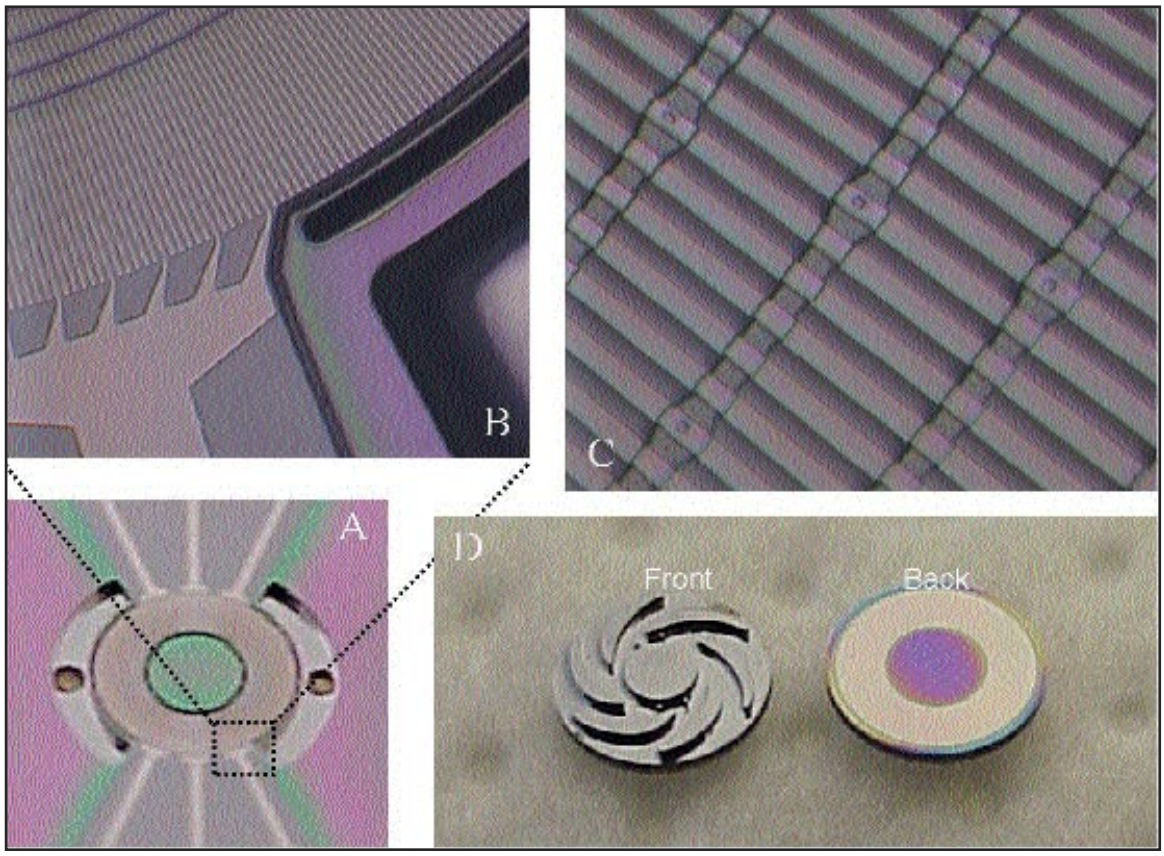

Microelectromechanical Devices

- *Sputter Deposition of Piezoelectric AlN Thin Films for Chemical and Biological MEMS Sensors*
- *Reliability of MEMS Devices in Shock Environments*
- *Residual Stress and Fracture in Thick Tetraethylorthosilicate (TEOS) and Silane-Based PECVD Oxide Films*
- *Microelectromechanical (MEMS) Thin Film Stress Sensors*
- *Anisotropic Silicon Trenches 300 μm Deep Employing Time Multiplexed Deep Etching*
- *Wafer-Level Packaging*
- *Micro Electric Machines for Micro Turbomachinery*
- *Micro Magnetic Machines for Micro Turbomachinery*
- *Implementation of a Self-Acting Thrust Bearing for a Silicon Micro Gas Turbine Engine*
- *Integrated Chemical Fuel Microprocessor for Power Generation in MEMS Applications*
- *Microchemical Reactors*
- *Microfabricated Devices for Biofermentation Studies*
- *Development of Hydrocarbon-Fueled Silicon Combustors for Power MEMS Applications*
- *Demonstration of a Microscale Heat Exchanger for a Silicon Micro Gas Turbine Engine*
- *Microfabricated Cell Analysis Device*
- *Micro-Hydraulic Transducer Technology*
- *Vibration-To-Electric Energy Conversion*
- *The Polychromator: A MEMS Correlation Spectrometer*
- *Dynamical Macro-Models for Magnetic MEMS Devices*

Sputter Deposition of Piezoelectric AlN Thin Films for Chemical and Biological MEMS Sensors

Personnel

W. Mao (R. Reif)

Sponsorship

C. S. Draper Laboratory

Low-temperature deposited Aluminum Nitride (AlN) thin-films can be used in many novel integrated devices including biological and chemical MEMS sensors. AlN is advantageous for MEMS use, because it can be deposited at low temperatures, is easily patterned using conventional photolithographic techniques, and is CMOS compatible.

0.5μm AlN films are deposited on SOI wafers from which flexural plate wave gravimetric sensors are fabricated. Sensor function involves using interdigitated transducers which act on the piezoelectric AlN layer to launch and detect flexural plate waves across a thin Si membrane. The Si membranes are coated with binding-site specific polymers; exposure to target chemicals results in an increase in membrane mass. This mass change is detected as a change in the membrane resonant frequency.

Previous work at MTL in support of the Draper Laboratory chemical and biological sensor project has resulted in a working protocol for the deposition of 0.5 μm low stress piezoelectric AlN films and a greater understanding of the relationship between film properties and deposition parameters. Further research toward understanding the mechanisms controlling film growth and properties is also necessary in order to have the capacity to produce films of similar quality in other sputtering systems. As device design and specifications change, it is crucial to maintain production of high quality films that are an integral component of the Draper chemical and biological sensors. Deposition of piezoelectric AlN thin films onto glass and ceramic substrates will also be investigated for increasing the flexibility of fabricating the Draper chemical and biological sensors and could also open the door to many new MEMS applications.

Reliability of MEMS Devices in Shock Environments

Personnel

S. Vengallatore and M. Kayahara
(S. D. Senturia)

Sponsorship

NSF

Microsystems can experience shock loading during fabrication, deployment, or operation, and are susceptible to failure by fracture, delamination, and stiction. We have developed a framework to analyze the dynamical reliability of MEMS based on:

(i) estimation of the mechanical response and

(ii) formulation of appropriate failure criteria.

MEMS are modeled as microstructures supported on elastic substrates, and the shock loads are represented as pulses of acceleration applied by the package on the substrate over a finite time duration. The relevant time scales in the response are the acoustic transit time, the time period of normal mode vibrations, and the duration of the shock load. For typical microsystems and loads (durations in the range 50 μs to 10 ms), we find the response of the substrate to be closely approximated by rigid-body motion. For a given microstructure attached to such a substrate, we have obtained time-domain criteria to identify those shock environments in which the stresses in, and deformations of, the microstructures can be estimated using quasi-static analyses. Based on a scaling argument, we have concluded that most cases of MEMS devices subjected to shock loading fall in the quasi-static or resonant-response regimes, and that the quasi-static fracture strength of a structure (or equivalently, the quasi-static fracture toughness of a material) is an adequate failure criterion

To support this analytical study, Kayahara has fabricated a variety of fracture-test microstructures using deep-reactive ion etching through a silicon wafer. The distribution of loads required to fracture one set of specimens will be used to predict the distribution of fracture loads of a related set of differing geometry. In parallel with this study, we have conducted fracture tests on the Polychromator (see "The Polychromator: A MEMS Correlation Spectrometer"). The applied shock loads have amplitudes in the range 1500g to 3500g, and durations varying from 0.3 ms to 1 ms. The micromachined polysilicon beams in the device were found to be immune to shock-induced failures, consistent with the predictions of the analytical framework. At present, we are evaluating the reliability of various components of the packaged device including the CaF_2 windows, the die-attach adhesive, and the wire-bonds.

Residual Stress and Fracture in Thick Tetraethylorthosilicate (TEOS) and Silane-Based PECVD Oxide Films

Personnel

X. Zhang and K-S Chen
(M. A. Schmidt and S. M. Spearing)

Sponsorship

ARO and DARPA

Plasma enhanced chemical vapor deposition (PECVD)

is an important thin film process for the fabrication of microelectronic devices and MicroElectroMechanical Systems (MEMS). Because PECVD is facilitated by plasma rather than by high temperature, it is widely used in applications with low thermal budgets or requiring fast deposition rates. Recent MEMS devices such as micromotors are pushing electrical and mechanical power requirements to higher levels. Higher power applications require thicker deposited layers, for example as electrical insulation or mechanical flexures. However, the ability to deposit films with thicknesses significantly greater than a few microns is limited by residual stress, which can result in substrate distortion or even cracking of the film or substrate. These stress problems increase with film thickness.

The present work was motivated by the process integration of a micro-motor driven compressor device. The micro-motor must have high power density and must operate at high efficiency. This places several requirements on the electrical stator. First, it must operate at high voltages (~300 V) without electrical breakdown. Second, the electrodes and interconnects must be well insulated from the substrate to minimize capacitive loading. Finally, the process must lead to a planar, unbowed surface to permit wafer bonding and to ensure a 3 μm air gap between the rotor and stator.

To meet these requirements, the stator electrical elements must be fabricated on top of a thick, high quality oxide film. To achieve this, two goals in film fabrication had to be met. First, sufficient thickness (typically, greater than 10 μm) was required in order to reduce capacitive loading. Second, the breakdown strength of the insulating film had to be able to withstand the high applied electrical loads. In order to achieve the first goal, PECVD oxides were chosen for the high deposition rate. After deposition, oxide films were subjected to a high temperature (typically 1100°C) densification to achieve better electric breakdown strength. Depositing oxide films with the required thickness was not difficult; however, after densification, the wafer exhibited excessive distortion and cracks were found in the film if the film thickness exceeded 15 μm. The deleterious effects of residual stress that tend to increase with thickness are a prime limitation to the deposition of very thick films. Since wafer distortion and film cracking both seriously impact MEMS process integrity and device reliability, it is important to elucidate the factors contributing to residual stresses in oxide films and to optimize the deposition process so as to reduce wafer bow and to avoid film cracking.

The present work focused on the residual stress characterization and fracture analysis in thick TetraEthylOrthoSilicate (TEOS) and silane-based PECVD oxide films. Conformality of TEOS-based oxide in high aspect ratio features has been found to be better than that achieved by other means of growing/depositing oxide. The aim of this work is to provide a fundamental understanding on the restress behavior and fracture mechanics of thick oxide films. Residual stress characterization and fracture analysis of thick silane and TEOS-based PECVD oxide films were conducted in order to understand the controlling mechanism for wafer bow and cracking in thick oxide films and to propose engineering solutions for the design of fabrication processes. Residual stress in oxide films was found to increase considerably upon thermal annealing. Given that the surface analysis of oxide films shows two orders of magnitude difference in hydrogen concentration before and after annealing, it is likely that the hydrogen gases played an important role in governing intrinsic stress. Both thick silane and TEOS-based oxide films were observed to crack after being exposed to the annealing cycle; the tendency to form cracks increased with film thickness and annealing temperature. Mixed mode fracture mechanics was applied to evaluate the critical cracking temperature, and experimental results indicated that the theoretical

Continued

Continued

prediction and test data are highly correlated. Finally, several engineering solutions were proposed and demonstrated to overcome the inherent physical problems associated with wafer bow and film cracks. Most importantly, the proposed engineering solutions not only allowed the specific process integration of a micromotor driven compressor device, but also provide important insights for the design of fabrication processes for other MEMS devices that require high temperature processing of dielectric films.

Microelectromechanical (MEMS) Thin Film Stress Sensors

Personnel

S. Seel, R. Bernstein, Y.H. Lau, M.J. Kobrinsky, E. Deutsch, K.P. Liew, and S. Lahiri (S.D. Senturia and C.V. Thompson)

Sponsorship

NSF and SRC

We have designed and fabricated two types of MEMS devices for the measurement of stresses in films during deposition and *in-situ* annealing. One class of devices uses micromachined single crystal microcantilevers with three resistors and one piezoresistor in a Wheatstone bridge fabricated in the cantilever. Piezoresistance measurements will be used to determine cantilever stresses resulting from stresses in films deposited on the cantilevers. The second type of device is based on the use of polysilicon fixed-fixed beams or cantilever beams in capacitor configurations in which the beams can be electrostatically "pulled-in" to the substrate. It has been shown that the pull-in voltage of microbeam structures is a strong function of the dimensions of the device, and of the modulus and stress state of the beams. We have extended analyses of the pull-in process for fixed-fixed and cantilever beams to account for the effects of films deposited on the beams. Determination of pull-in is being extended to electrical detection and capacitive detection from the current optical detection, which will make *in-situ* measurements possible. We have demonstrated in experiments that fixed-fixed beam structures can be used to measure stresses of less than 3MPa in 1000nm-thick films and less than 30MPa in 100nm-thick films. Cantilever piezoresistor and modified pull-in structures are expected to have substantially higher sensitivities. Our new pull-in structures will be compatible with *in-situ* use in sputter depositions.

A third device is based on the buckling of a silicon dioxide/silicon membrane. The amount of buckling depends on the stress in the membrane, and can be measured very accurately using a Wyko Optical Profiler. The addition of another thin film on the membrane changes the buckling state of the membrane, in a way that reveals the average stress in the deposited film. These devices can be used in chip form, or as a complete wafer for characterization of the stress variation across a wafer. These devices should be particularly useful for characterization of films deposited using

Continued

Continued

Chemical Vapor Deposition (CVD). CVD processes lead to deposition on both sides of cantilever beams, and therefore leads to a compensating effect on beam curvature. However, films deposited on both sides of a buckled membrane lead to an additive effect on the buckling state. We are developing devices compatible with *in-situ* use in CVD systems.

Membrane devices will also be used for studies of stress evolution during nickel silicide formation.

Anisotropic Silicon Trenches 300 μm Deep Employing Time Multiplexed Deep Etching

Personnel

X. Zhang, R. Khanna, and A. A. Ayon
(M.A. Schmidt)

Sponsorship

ARO and DARPA

This work reports solutions to the problem of profile control of narrow trenches in the vicinity of wider topographic features, as well as for etching high aspect ratio, anisotropic trenches with depths in the 300 to 500 μm range, and of widths between 12 to 18 μm. Additionally, specific operating conditions are discussed to address uniformity variations across dies with diameters in excess of 4200 μm.

Deep Reactive Ion Etching (DRIE) is being increasingly recognized as an enabling MEMS technology and it is, in fact, playing a crucial role in the emerging field of Power MEMS. An extensive characterization database has been reported recently for tailoring operating conditions in order to obtain prescribed profiles as well as targeted silicon etching rates and uniformity when using a DRIE tool that employs the Bosch process. This technique can be briefly described as consisting of sequential etching and passivating steps using an appropriate gas chemistry in each step (SF_6 for etching, C_4F_8 for passivating). However, solutions to the problem of etching high aspect ratio trenches located in the vicinity of wide trenches that locally deplete the availability of etching species are absent in the literature. Furthermore, the issue of etching highly anisotropic, narrow silicon trenches (measured widths of 12 to 18 μm) with etched depths in the range of 300 to 500 μm has not been scrutinized and no reported practical guidance can be found in this respect. Additionally, it is possible to locate in the literature suggested approaches to improve etching uniformity, however, the need remains to obtain and compare observations in specific cases.

The mask used in these experiments consists of an array of 12 circular trenches with a diameter of 4200 μm and measured width of 10 μm after photolithography. Standard vacuum theory applied to narrow (width ≤ 13 μm), very high aspect ratio (>15) silicon trenches, reveals that the conductance of these features decreases as the depth of the trench increases. Decreasing the conductance of the trench impedes both

Continued

Continued

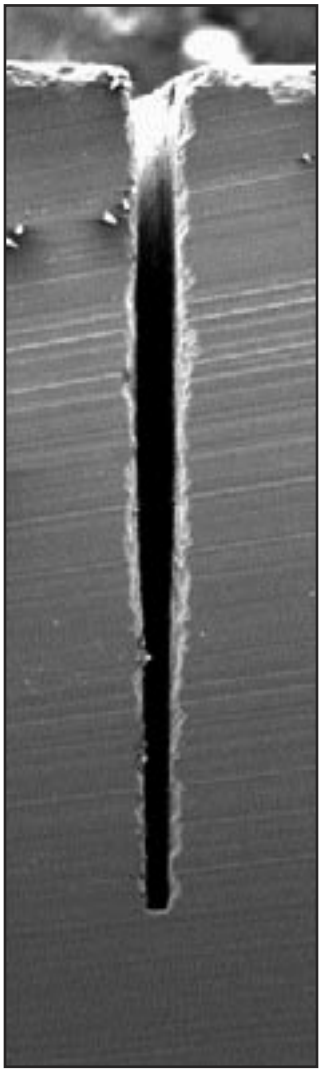

Figure 1. Trench profile quickly deteriorates as the depth of a high aspect ratio trench increases. The trench in the left SEM micrograph was obtained during a 4-hour etch using MIT56.

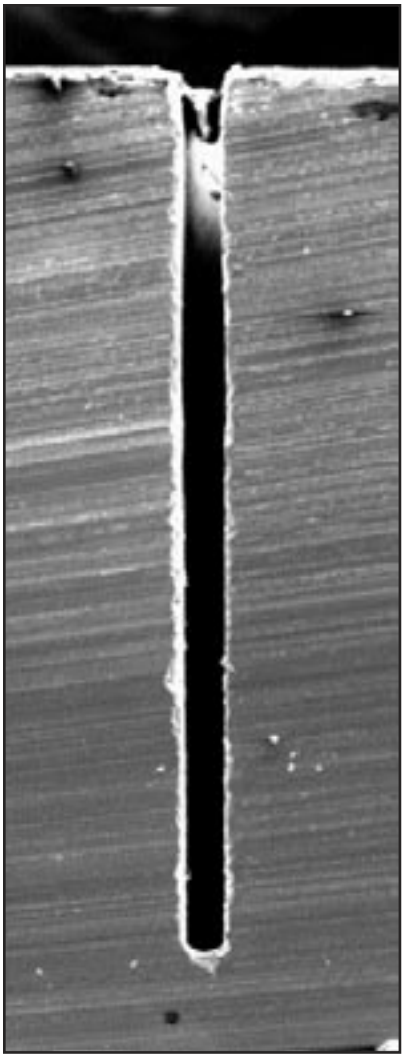

Figure 2. Operating conditions are based on MIT56, with +2 sccm increase in SF_6 flow rate every hour. The average width of the trench is about 11.8 mm. Normally, a 4-hour etch delivers a 315-320 mm deep trench.

Continued

Continued

the transport of etchant species to the surface bottom and the removal of etching byproducts. The combined effect is reflected in the noticeable profile deterioration when depth increases beyond 200 mm, as shown in Figure 1.

This problem can be alleviated by dynamically compensating the neutral flux reduction reaching the feature bottom during processing and by quickly removing the etching byproducts that dissociate and redeposit. This type of control is natural in tools employing the Bosch process because in the standard mode of operation, the throttle or Automatic Pressure Control (APC) valve remains fixed and the chamber pressure is controlled by the flow rate of the respective gas species during the etching or passivation cycles. Thus, the pressure during the etching cycle can be systematically increased throughout a particular process simply by increasing the SF_6 flow rate. Additional advantages of operating at higher pressures include higher collision and dissociation rates that increase the availability of etching species. The higher SF_6 flow rates associated with high-pressure operation facilitate the replenishing of etching species and the quick removal of etching byproducts. Thus, increasing the SF_6 flow rate was the approach selected to locate processing conditions that permitted the repeatable microfabrication of trenches with depths in excess of 300 μm, with measured widths ≤ 13 μm and good profile control, as the trench shown in Figure 2.

Wafer-Level Packaging

Personnel

C. Tsau
(M.A. Schmidt and S.M. Spearing)

Sponsorship

DARPA

Packaging costs often dominate the total cost of a system based on MEMS devices. Thus, tremendous cost leverage is possible by addressing fundamental changes in the methods of packaging of MEMS devices. We are pursuing wafer-level packaging approaches that take advantage of the economy of batch fabrication. In other words, when the packaging is accomplished at the wafer level, the cost of that packaging operation is distributed over the 1000+ devices on the wafer, thus significantly lowering cost.

We are exploring the fundamental properties of a wafer-level thermocompression bond. This bond is performed by pressing two silicon wafers with thin patterned gold films together in such a way that the gold films deform and bond. The bond is performed at 300-350C, permitting it to be performed after integrated circuits and MEMS devices have been formed on the wafer. In addition, because the bond layers are conductors, the bonding layers may also be used for local sig-

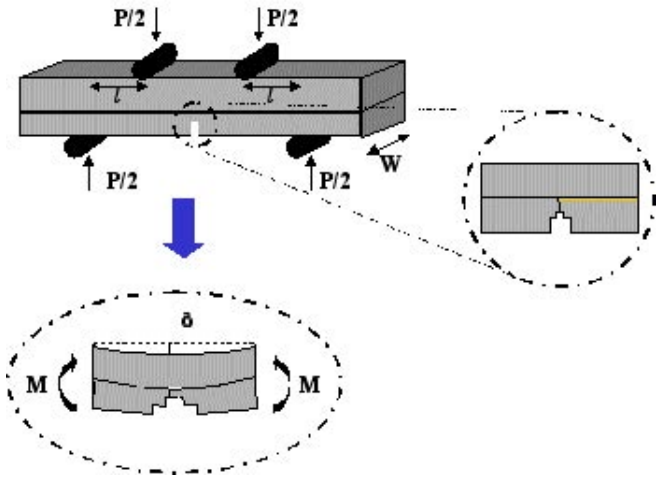

Fig. 3: 4-pt Bending Configuration

Continued

Continued

nal routing. Lastly, it is possible that the bonding can be performed in a vacuum, which can be critical to the operation of some inertial sensors.

Thus far, we have established a wafer-level bonding protocol for 4" wafers using a commercial bond tool (Electronic Visions). Additionally, we have developed a bond strength measurement technique which permits a direct measure of the de-bond energy. The technique utilizes a four point bending configuration in which the load deflection characteristics of a bonded sample are measured as a crack propagates along the bonded interface. A load plateau is measured, from which the bond strength is extracted. Ongoing work include mapping the bond quality over a range of process conditions, bonding in vacuum, and assessing the local interconnect capability of the bond.

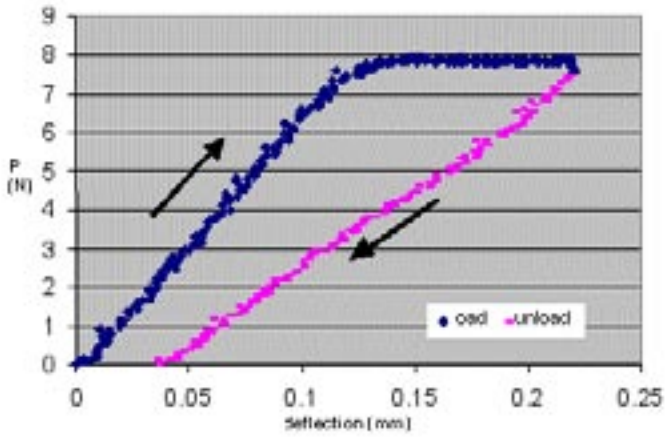

Fig. 4: Measured load-deflection characteristics indicating crack propagation.

Micro Electric Machines for Micro Turbomachinery

Personnel

C. Livermore, J. H. Lang, S. D. Umans, E. P. Warren and X. Zhang in collaboration with (A. H. Epstein, M. A. Schmidt, S. D. Senturia, and A. Forte of MIT Lincoln Lab)

Sponsorship

ARO and DARPA

This project is part of the MIT Micro Gas Turbine Engine Project. The MIT Micro Gas Turbine Engine Project has the goal of using MEMS fabrication technologies to construct compact electric power generation systems from a gas turbine generator comprising a compressor, combustor, turbine and electric generator. Other systems under development include stand-alone motor/compressors and turbine/generators. The MIT Micro Gas Turbine Engine Project is highly interdisciplinary, involving students, staff and faculty from several academic departments and laboratories.

This project seeks to develop the motors and generators employed in the micro turbomachines mentioned above, and to develop their power and control electronics. Following the analysis of several candidate machine types, the electric induction machine was selected for these applications. This electric machine is a disk-shaped axial-field machine, and is shown in edge view in Figure 5. On one side of its air gap, polysilicon stator electrodes are supported by a thick silicon-dioxide insulator buried in a substrate. The electrodes are connected to form one or more phases, and are excited so as to impose a potential wave which travels around the stator. On the other side of the air gap is the rotor, which rotates as a disk. The rotor consists of a conducting polysilicon film supported by a silicon-dioxide insulator buried in a substrate. Photographs of an actual stator and rotor are shown in Figure 6.

During motoring operation, the power electronics excite the stator electrodes to produce a potential wave which travels around the stator with a speed exceeding that of the rotor. This wave, and the corresponding charges which reside on the stator electrodes, induce image charges on the rotor surface across the air gap. Since the speed of the traveling potential wave exceeds the mechanical speed of the rotor, convection alone cannot synchronize the rotor charges with the traveling wave, as must happen in steady state. Thus, the rotor charges must conduct through the rotor film to main-

Continued

Continued

tain synchronism. The conduction process must in turn be driven by a tangential electric field, and so the rotor charges lag behind the potential wave to produce that field, as shown in Figure 5. Finally, the tangential electric field acts on the rotor charges to impart a tangential surface stress on the rotor, which in turn results in a motoring torque. During generating operation, the rotor speed exceeds that of the traveling potential wave, and the torque is reversed.

To date, detailed models of the electric induction machine have been developed and used to design an optimized 6-phase machine having a 4-mm diameter. As a motor, this machine is expected to produce a 3-W mechanical output at 2.4 Mrpm when its phases are excited with 300-V 3-MHz sinusoids. Recently, two such motors were fabricated and tested with low-voltage stator excitations. One motor, described in *[S. F. Nagle, "Analysis, Design and Fabrication of an Electric Induction Micromotor for a Micro Gas-Turbine Generator", PhD Thesis, MIT EECS Department, October 2000*], was a tethered motor. In this motor, the rotor was stationary, and was supported by mechanical tethers, or springs. The bending of the tethers was used to accurately measure torque. The other motor was built into a motor compressor, and is described in [*L. Frechette, "Development of a Micro-Fabricated Silicon-Motor-Driven Compression System", PhD Thesis, MIT AA Department, August 2000*]; (see Figure 6). In brief summary, both motors performed essentially as expected given their low-voltage excitation.

Our work now focuses on the fabrication and testing of a generator to be mounted on the compressor shroud of the micro gas turbine engine. The primary challenge of this work is fabrication: devising fabrication flows and techniques for the generator, and fabricating the actual machine. This is made difficult by the two-level interconnected metal structure that will be the low-resistance electrical stator. Because this stator must survive high temperatures during both fabrication and operation, it uses a two-level platinum structure with deposited oxides for the interlayer dielectric. With such a stator the net output power from the generator system,

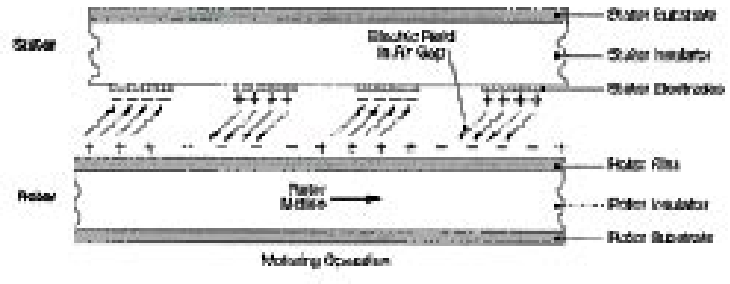

Fig. 5: A: edge view of the electric induction machine.

Continued

is expected to be approximately 0.5 W; demonstration is expected later this year.

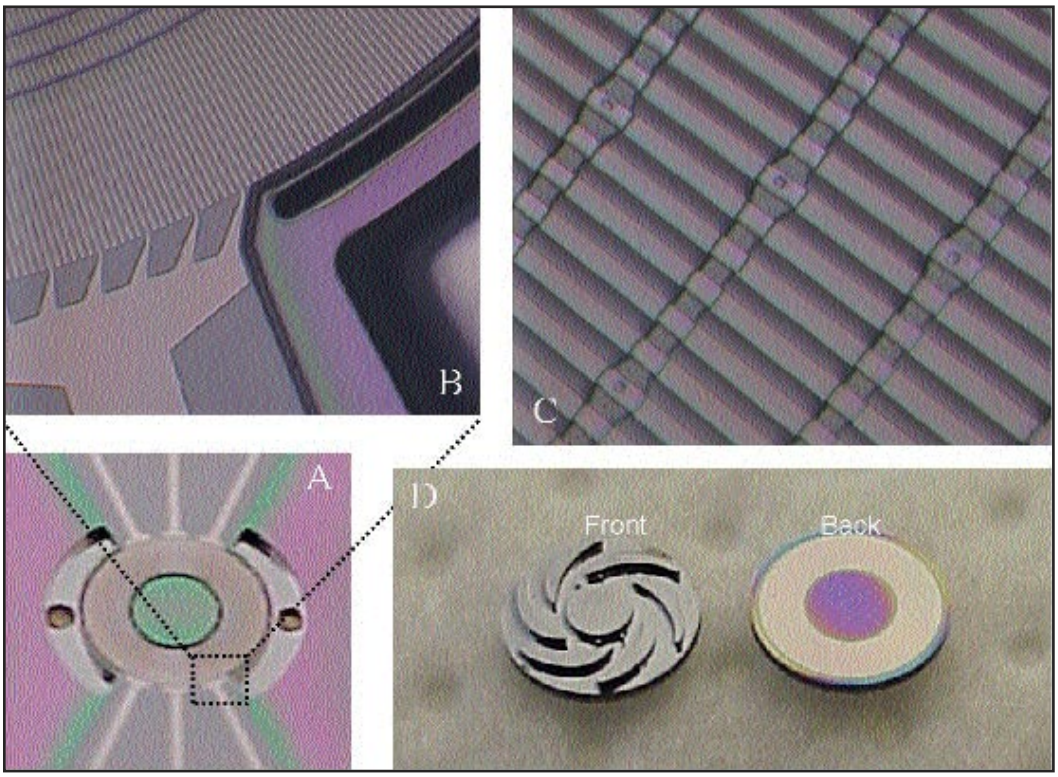

Fig. 6: Photographs of a micro electric induction motor used in a motor compressor: (A) a wide view of the stator; (B) a close up view of the stator showing the outer edge of the stator electrodes and their connections to one phase lead; (C) a close up view of the stator electrodes showing the interconnection of electrodes of the same phase through buried interconnect rings; (D) the front side of the rotor showing the compressor blades, and the back side of the rotor showing the rotor conductor.

Micro Magnetic Machines for Micro Turbomachinery

Personnel

H. Koser (J. H. Lang in collaboration with S. D. Senturia and A. H. Epstein, and M. Allen and F. Cross at the Georgia Institute of Technology)

Sponsorship

ARO and DARPA

This project is part of the MIT Micro Gas Turbine Engine Project. The MIT Micro Gas Turbine Engine Project has the goal of using MEMS fabrication technologies to construct compact electric power generation systems from a gas turbine generator comprising a compressor, combustor, turbine and electric generator. Other systems under development include stand-alone motor/compressors and turbine/generators. The MIT Micro Gas Turbine Engine Project is highly interdisciplinary, involving students, staff and faculty from several academic departments and laboratories.

The first generation of motors and generators under development for the micro turbomachines mentioned above are electric as opposed to magnetic in nature. In contrast, this project seeks to develop alternative machines that are magnetic, specifically magnetic induction machines. These machines will be fabricated from electroplated cores and conductors using facilities at the Georgia Institute of Technology maintained by Professor Allen and his students, who are collaborators in this project. The main reason for pursuing magnetic induction machines, despite their increased fabrication complexity, is that they can operate with much wider air gaps thereby reducing windage losses. They also appear to be capable of providing a greater power and torque density than their electric counterparts, and the development of their associated power electronics appears to be less challenging.

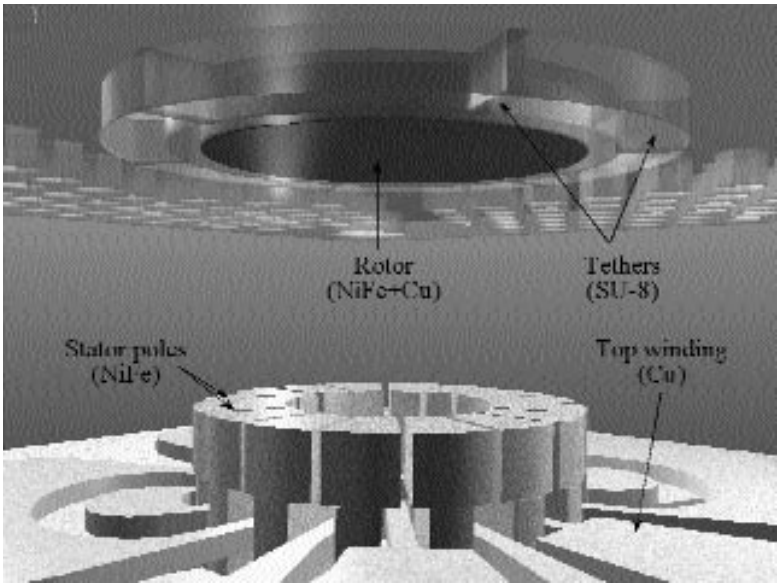

Fig. 7: An expanded view of a tethered micro magnetic induction motor showing the rotor above and the stator below.

To date, detailed models of the micro magnetic induction machine have been developed and used to design 2-phase axial-gap planar motors having a 4-mm diameter. Based on these designs, fabrication flows which utilize the electroplating facility at the Georgia Institute of Technology have also been developed. Finally, tethered motors, which serve as torque measurement devices have been fabricated, and testing is now underway. An expanded drawing of an electroplated tethered motor is shown in Figure 7. The upper half of the figure shows a Cu conducting film deposited on a NiFe rotor suspended by epoxy tethers. During operation, torque is measured through the bending of the tethers. The lower half of the figure shows the stator which comprises a NiFe core and two phase Cu windings that pass through slots in the core.

Implementation of a Self-Acting Thrust Bearing for a Silicon Micro Gas Turbine Engine

Personnel

C. W. Wong, X. Zhang, and S. A. Jacobson
(M. A. Schmidt and A. H. Epstein)

Sponsorship

ARO and DARPA
As part of a program to produce a self-contained micro

gas turbine engine, we present the design and fabrication of a self-acting thrust bearing microfabricated from silicon. Comprising of 2.2 μm deep by 40 μm wide spirals across a diameter of 700 μm, these microstructures provide high stiffness capabilities, elimination of external bearing pressurization, and considerable reduction of complexity in system microfabrication.

Reported widely in the 1960s bearings literature and used commonly in seals, we introduce hydrodynamic spiral grooves into the microscale regime. These self-acting spiral grooves function by viscous pumping of fluid into the thrust bearing, an effect introduced by and dependent on the rotational motion of the rotor - as a result, large stiffness is possible with high rotational rates. In contrast, hydrostatic thrust bearings, which typically consists of a restrictor orifice and an outflow lubrication film, rely on an external pressurization source to provide the necessary stiffness.

Our design involves an optimization of the geometric parameters against the design trade-off of axial stiffness and load capacity. Included in the constraint is also the need to implement this design with minimal changes to the overall system design. Parameters of concern are the spiral groove angle, groove width and depth, fluid film gap, number of spirals and diameter of the thrust bearing. The resulting design predicts a 0.07N load capacity and a 120,000N/m axially-centered stiffness at 200,000rpm, sufficient to "lift-off" the rotor under our experimentally derived operating conditions. Dynamic stability and rarefaction effects of the thrust bearing are also modeled in order to obtain feasible operation up to 1.2×10^6rpm.

Our design choice of minimal changes to the current devices, however, produces a low thrust bearing stiffness during start-up operation of the rotor. We thus included an additional hybrid design that allows for temporary hydrostatic pressurization to investigate the hydrodynamic spiral groove effects at higher rotational speeds. In addition, if we are not limited by the current build of test devices, sufficient stiffness during start-up operation could be simply provided by increasing thrust bearing diameter, a parameter that has minimal effects on the overall system design.

The test structure consists of a five-wafer stack, with the second and fourth wafer containing the spiral grooves with crucial dimensions. The fabrication process for these two wafers are similar and involves four shallow reactive ion etches and two dry anisotropic deep reactive ion etches to define the components. Challenges in fabrication include tight tolerances on two such shallow etch depths, upon which the stiffness is strongly dependent. The completed thrust bearings wafers are then aligned and thermally bonded with the rest of the wafers to form the wafer stack. Experiments on a hybrid bearing suggest a hydrodynamic stiffness as slightly lower than predicted. A purely hydrodynamic aft thrust bearing device is tested and the effects of the spiral grooves analyzed. Finally transition to hydrodynamic operating mode for a hybrid bearing is demonstrated.

Integrated Chemical Fuel Microprocessor for Power Generation in MEMS Applications

Personnel

L. Arana, A. Franz, O. Nielsen, and S. Schaevitz
(K.F. Jensen and M.A. Schmidt)

Sponsorship

DARPA

This program is investigating a variety of chemical fuel microprocessors that could be used for power generation. Such power generators would be used as replacements for batteries, and potentially offer superior performance when compared to batteries due to the high energy content of fuels. The program has three thrusts. The first is to investigate reactors that would generate hydrogen for fuel cells. The second is to optimize previously developed membrane technology for hydrogen separation/purification as a critical enabling element of a fuel cell. The third is to investigate power generation methods utilizing either ThermoElectric (TE) and ThermoPhotoVoltaic (TPV) effects integrated with microreactors. A micromachined thermoelectric generator has been built using SiGe thermopile material and has yielded electric power.

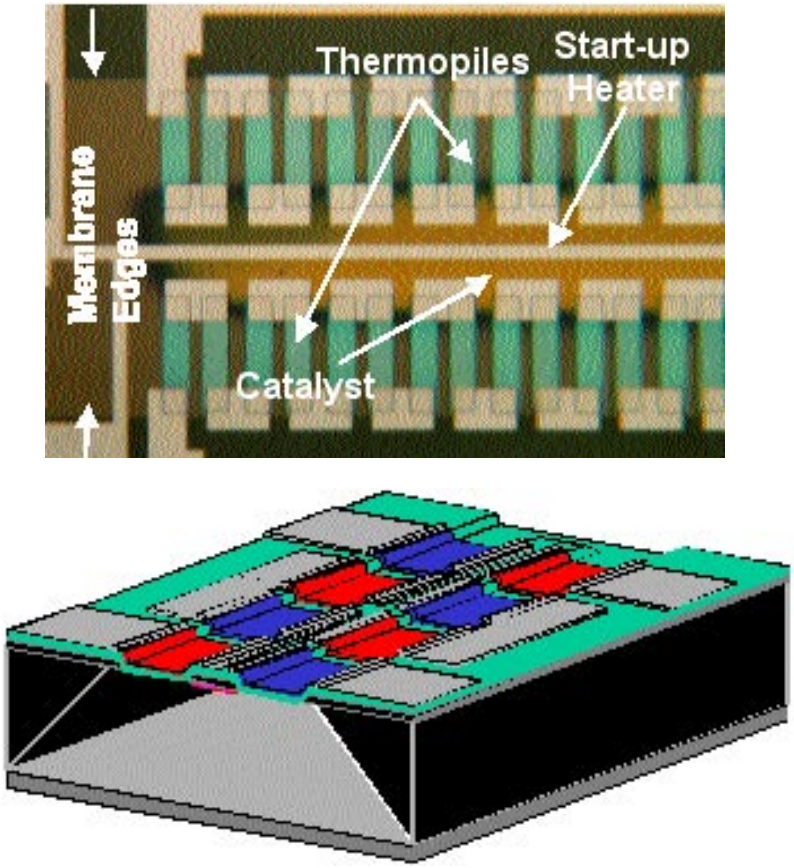

Fig. 9: A micromachined thermoelectric generator.

Microchemical Reactors

Personnel

S. Ajemera, N. DeMas, S.Firebaugh, T. Floyd, R. Jackman, M. Losey, H. Lu, and D. Quiram
(K.F. Jensen and M.A. Schmidt)

Sponsorship

DARPA

This program aims to explore methods and technologies for performing chemical reactions at the microscale. These microreactors can be applied for chemical screening (eg. catalysts) as well as for chemical synthesis. The benefits of microreactors can be many fold. Certain reactions will have better performance because of the much higher surface to volume ratio in miniaturized reactors. This is particularly true for highly exothermic reactions where heat removal is critical. Also, the small scale of these reactors, and the ability to configure them in parallel open opportunities for point of use chemical production systems in specialty chemical applications. Such an approach might offer advantages in eliminating expensive and risky shipping and storage issues, as well as permit tailoring of the plant output based on demand (e.g. for chemicals with seasonal demand). The scale-out approach mentioned above might also allow for a much more rapid time to market compared to the traditional chemical industry scale-up process. Finally, these microreactors can permit investigations of fundamental reaction kinetics that can't be observed in macroreactors.

The specific activities of the program involve; development and demonstration of novel reactors for gas-gas, gas-liquid, and liquid-liquid reactors, development of packaging and control approaches for reactor scale-out, optimization of microreactors through numerical analysis, and investigation of new sensing methods for reactor control.

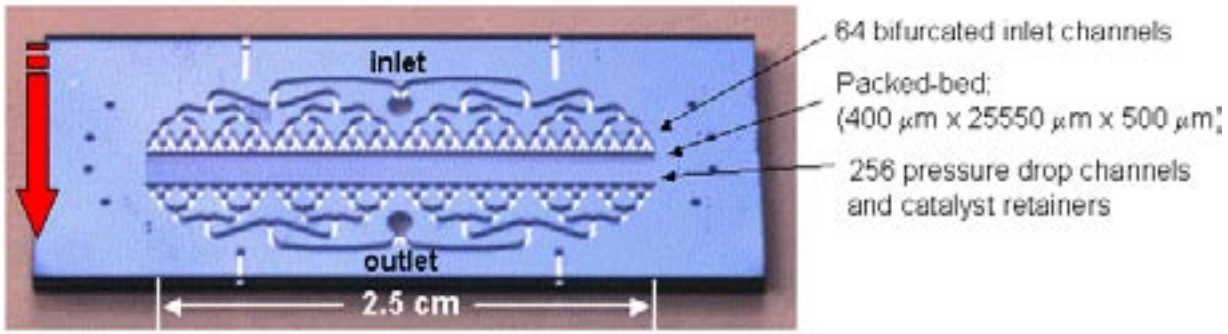

Fig. 9: A cross-flow packed bed reactor chip

Microfabricated Devices for Biofermentation Studies

Personnel
A. Zanzotto (K.F. Jensen and M.A. Schmidt in collaboration with Prof. P. Laibinis, Prof. R. Ram, and Prof. A. Sinskey)

Sponsorship
DuPont

This new program aims to explore the opportunities of applying microfabrication technology to the area of fermentation. Specifically, we will investigate novel microfluidic structures for fermentation. The technical challenges include design of the fermentors in such a way that the cells can be supplied with nutrients and properly agitated. Surface coatings/treatments are a critical component. Lastly, new methods and devices are needed for optical measurements *in-situ*.

Development of Hydrocarbon-Fueled Silicon Combustors for Power MEMS Applications

Personnel
C. M. Spadaccini, J. Lee, X. Zhang, and C. Cadou (I. A. Waitz)

Sponsorship
ARO and DARPA

Recent advances in the field of silicon micro-fabrication techniques and silicon-based Microelectromechanical Systems (MEMS) have led to the possibility of a new generation of micro heat engines for power generation and micro air-vehicle propulsion applications. The design for a silicon-based, micro gas turbine generator capable of producing 10-50 Watts of power in a volume less than 1 cm^3 while consuming 7 grams of fuel per hour has been developed. This represents a ten-fold increase in power density over the best available batteries.

An engine of this type will require a high temperature combustion system to convert chemical energy into kinetic and thermal energy. To accomplish this, a unique set of challenges must be overcome:

- Shorter residence time for mixing and combustion.
- Heat loss due to high surface area-to-volume ratio.
- Material and structural constraints of silicon.
- Rudimentary 3-D geometry due to limits of microfabrication techniques.
- Micro-engine thermodynamic cycle constraints.

All of the above impact the design and development of a suitable micro-combustion system.

The baseline device is comprised of all the non-rotating functional components of the micro gas turbine engine. The device measures 2.1 x 2.1 x 0.38 cm, and is aligned-fusion bonded from 6 silicon wafers. Figures 10 and 11 show a schematic and a SEM of this first micro-combustion system. Fabricated largely through Deep Reactive Ion Etching (DRIE), the structure required anisotropic dry etching through a total thickness of 3,800 μm. Complete with a set of fuel plenums, fuel injector holes, pressure ports, and compressor and turbine static airfoils, the design of the six-wafer structure

Continued

Continued

required a multi-disciplinary approach that accounted for all the chemical, structural, and fluidic interactions as well as engine system considerations.

For the propulsion and power generation applications of interest, the principal figure of merit is power density. The baseline device achieved power densities in excess of 2000 MW/m^3 with hydrogen-air combustion. This corresponds to exit gas temperatures over 1700 K and combustor efficiencies greater than 95%. These power densities are three to four times larger than those produced by a conventional gas turbine combustor and are an order of magnitude larger than other power MEMS device. Hydrocarbon fuels, such as ethylene and propane, have been burned in this device at lower power densities, 800 MW/m^3 and 500 MW/m^3 respectively.

To achieve higher power densities and efficiencies using hydrocarbon fuels, several new combustors are in development. The dual-zone micro-combustor is a simple modification to the six-wafer geometry, but represents a significant change in combustion strategy. A series of holes through the inner wall have been created connecting the upper cooling jacket to the combustion chamber, thus some of the inlet air will be diverted from passing into the combustor inlet. Air that bypasses the combustor inlet is then introduced in the middle of the combustion chamber to reduce the temperature of the hot combustion products to the desired turbine inlet temperature of 1600 K. This diversion increases the local equivalence ratio of the fuel-air mixture entering the combustion chamber to near stochiometric levels, increasing the temperature and thus, the kinetic rate. With this device, a 100% increase in power density was achieved for the same operating conditions as the six-wafer structure. Testing of this combustor is still in progress.

A combustor which utilizes heterogeneous catalysis to improve hydrocarbon-air reaction rates, has also

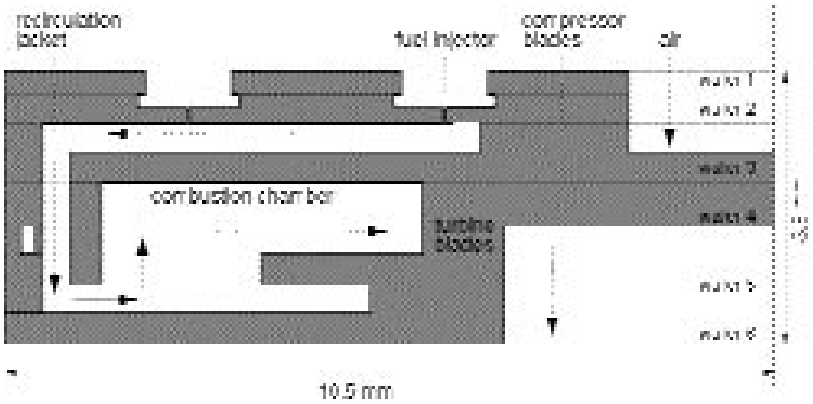

Fig. 10: Schematic of six-wafer combustion system.

Continued

been identified as a means of increasing power density. Initial tests with platinum coated nickel foam implanted into previously fabricated three-wafer combustors, were successful. Where hydrocarbon-air combustion could not previously be stabilized, ethylene and propane were both burned at approximately 1/2 the power density of hydrogen-air combustion in the same device. As a result, efforts are underway to fabricate a six-wafer device with platinum implanted inside the combustion chamber.

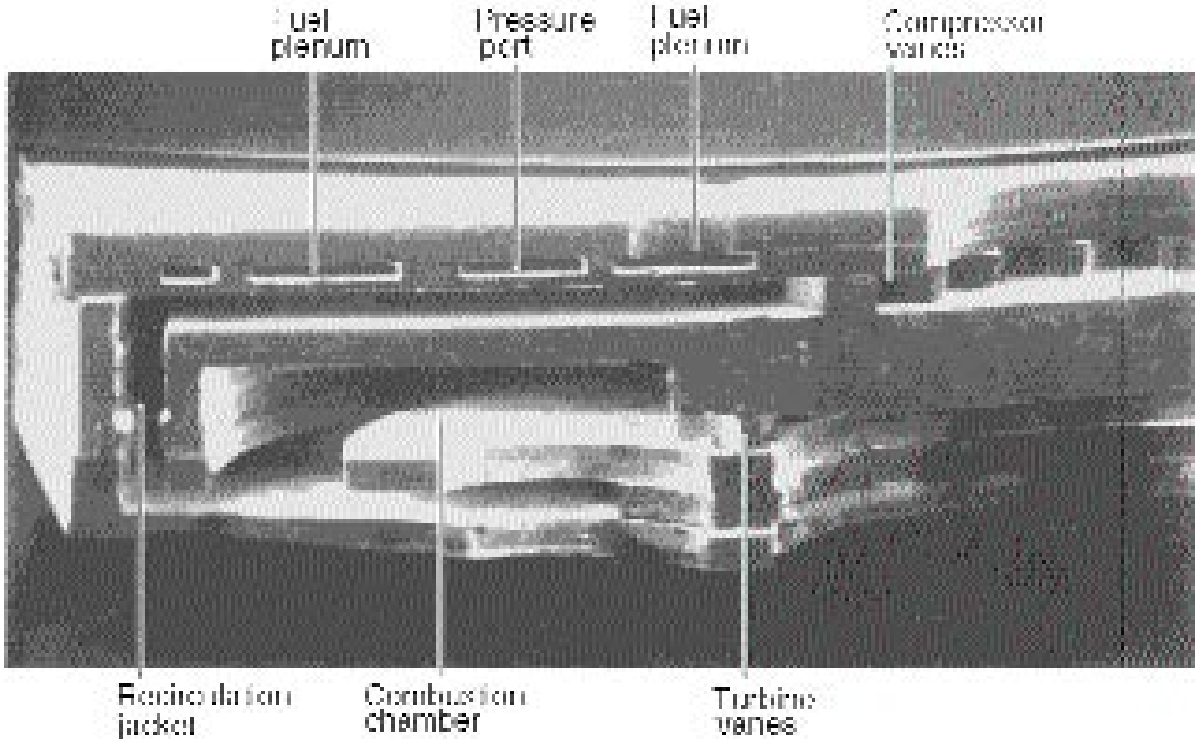

Fig. 11: SEM cross-section of six-wafer combustion system.

Demonstration of a Microscale Heat Exchanger for a Silicon Micro Gas Turbine Engine

Personnel

S. Sullivan, X. Zhang, and A. A. Ayon
(M. A. Schmidt and J. G. Brisson)

Sponsorship

ARO and DARPA

The design, fabrication, modeling, and testing of silicon counterflow heat exchanger for use in the MIT micro gas turbine engine is discussed. Although silicon is the preferred material in microfabricated devices, it is not the choice for recuperative heat exchanger applications. Its high thermal conductivity allows heat transfer between opposite ends of the device, reducing the overall effectiveness. Designing and fabricating a heat exchanger that can overcome this behavior poses several challenges.

The heat exchanger design consists of three wafers level bonded together. Included in the device were flow distribution and collection regions, and a layer that is characterized by an array of parallel heat transfer passages. The channels are 7 mm long, 40-90 μm wide, etched to a depth of 200 μm, and separated by 10 μm-thick walls. The flow distribution and collection regions are quite large (20 × 0.2 mm) and deep (150-200 μm), in order to maximize the flow area and to minimize the thickness of the remaining wafer.

As a parallel endeavor, techniques were investigated for utilizing other materials in the construction of recuperator structures. Several experiments were run to determine the feasibility of fabricating heat transfer passage walls out of silicon and silicon dioxide. Silicon dioxide was deposited on framework of silicon posts in order to create low thermal conductivity walls.

The heat exchanger's performance is characterized by two competing figures of merit; the effectiveness (a measure of its heat transfer), and the pressure drop. The effectiveness improves by increasing the surface area available for heat transfer, minimizing the thermal resistances between the two flows, and minimizing the cross sectional area available for axial conduction. The pressure drop improves by reducing the ratio of surface area to cross-sectional flow area. These competing requirements are further constrained by the limitations of microscale fabrication.

The primary obstacles to improving the performance of the heat exchangers is the depth the passages could be etched to, and how thin the silicon wafer could be made without it breaking. Increasing the depth of the channels improves both the pressure drop and the effectiveness, since it increases the available flow area while increasing the heat transfer surface area. Reducing the thickness of the remaining silicon wafer reduces the amount of cross sectional area available for axial heat transfer.

Heat exchangers with microscale features were successfully fabricated. The completed devices were packaged using Kovar tubing and then sealed using melted glass. Packaged heat exchangers were tested in an experimental setup constructed for this purpose. Preliminary testing produced data that was consistent with the predicted performance of the devices. For mass flow rates and pressures appropriate to the MIT micro gas turbine engine, the heat exchanger showed less than a 10% drop in pressure and an effectiveness of 0.6.

Microfabricated Cell Analysis Device

Personnel

R.A. Braff and J. Voldman
(M.L. Gray, M.A. Schmidt, and M Toner)

Sponsorship

NSF, Kodak, and NIGMS

Microfabrication technology has the unique capability of producing arrays of devices as well as devices that are of the dimensions of biological cells. In this project we are exploring methods for cell capture and release that leverage these capabilities and could be productively deployed in a miniature biological instrument for discovering basic biological processes. Two approaches are being investigated for cell capture and release.

The first uses DielEctroPhoretic (DEP) forces. DEP forces can be used to create non-contact traps for capturing single particles such as cells. We have developed modeling tools with which we can design high-performance traps that can capture and hold cells under strong flows. These high-performance traps employ a novel three-dimensional extruded geometry. With these traps we can capture, hold, and electrically release single cells with single-trap control. We plan to now use arrays of these traps to perform biological assays.
The second uses hydraulic forces generated by MEMS actuators for cell manipulation. Thin film platinum heaters are used to form water vapor bubbles that serve

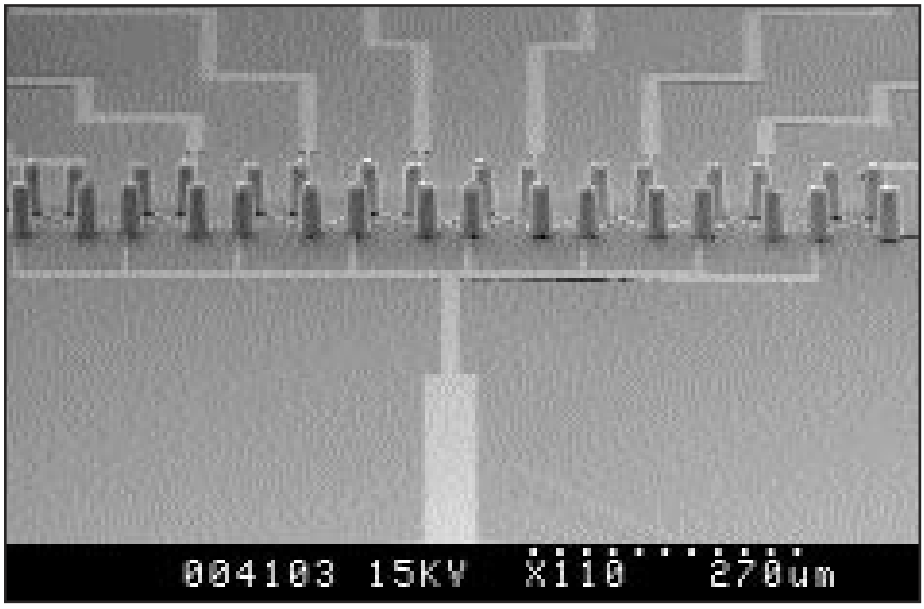

Fig. 12: This scanning electron micrograph shows a completed 1x8 array of cell traps. Each trap consists of four extruded gold electrodes fabricated by electroplating.

Continued

as the means of actuation. We are currently studying microbubble formation and developing ways by which the bubbles can be more controllable and predictable. Once this has been accomplished we plan the use the bubbles as the actuation mechanism for the manipulation of biological cells.

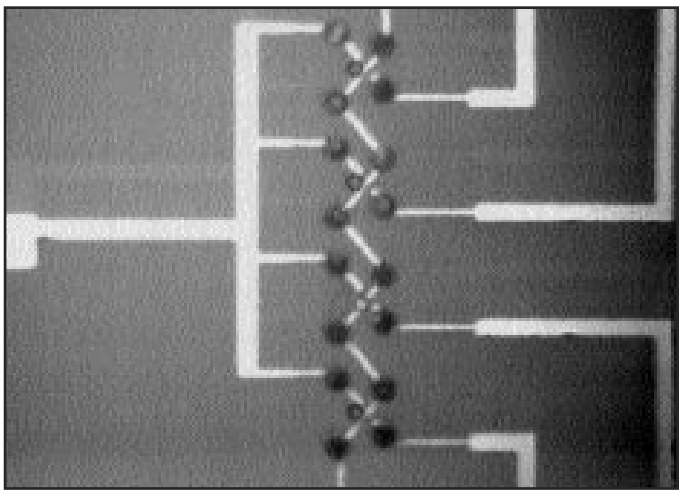

Fig. 13: Top-down view of the cell traps in action. The traps are placed in a flow chamber and filled with liquid containing beads. When turned on, the beads are captured in the individual traps. In this photo, four traps each contain one latex bead.

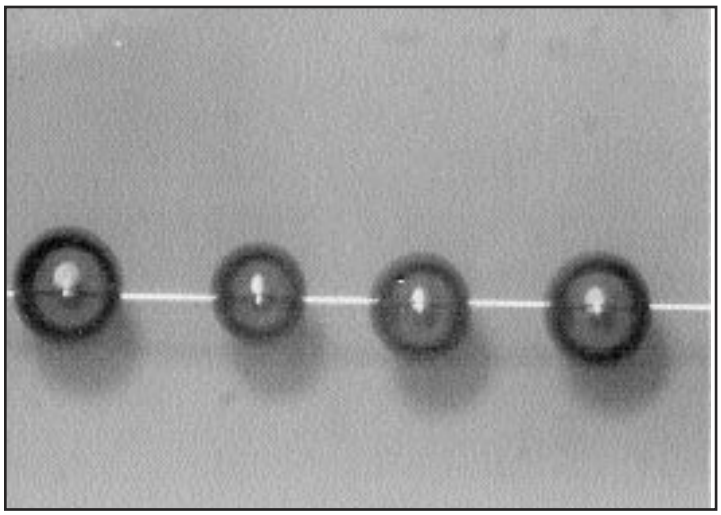

Fig. 14: Microbubbles formed on a platinum heater.

Micro-Hydraulic Transducer Technology

Personnel

J. A. Carretero, H.Q. Li, R. Mlcak, D.C. Roberts, L. Saggere, J.L. Steyn, Y.-H. Su, K.T. Turner, and O. Yaglioglu
(N.W. Hagood, M.A. Schmidt, S.M. Spearing, and K.S. Breuer)

Sponsorship

DARPA and ONR

The objective of this program is to develop highly compact (15mm×15mm×5mm) miniature transducers called Micro-Hydraulic Transducers (MHT) that are capable of outputting energy at very high power density (>1 kW/kg). The MHT technology exploits from the integration of the enabling micromachining technology with piezoelectric technology and microhydraulic concepts.

The MHT device is comprised of the following generic components: pump chamber enclosing a piezoelectric element, two actively controlled piezoelectrically driven valves, a Low-Pressure fluid Reservoir (LPR), and a High-Pressure fluid Reservoir (HPR). The two active valves – one operating between the LPR and the harvesting/pump chamber and the other one operating between the pump chamber and the HPR - regulate the fluid flow into and out of the harvesting/pump chamber. The generic configuration of an MHT system is such that the device can be operated as both an actuator that supplies high mechanical force in response to electrical input and as an energy generator that transduces electrical energy from wasted mechanical energy in the environment. In the actuator mode, the working fluid flows from LPR to HPR via the pump chamber, and in generator mode, the fluid flows in the reverse direction. The piezoelectric element within the pump chamber serves as the main energy transducing element. The MHT devices find many novel applications. As actuators, the MHT devices can be used to effect large force/strain in active structural control applications and as compact drives in miniature robotics. As energy generators, the transducers can extract electrical energy from wasted mechanical energy sources such as vibrations of operating machinery and the heel strike of human gait.

The current research efforts are primarily focused towards developing a heel-strike energy generator, an entirely self-contained device fitting in the heel of a soldier's boot, that can generate and store energy from the soldier's ambulatory activities. Fabrication and testing of the main components of the transducer are currently underway. A first generation drive component incorporating a PZT-5H piezoelectric element that is common to both the pump and the active valve chambers has been successfully fabricated and tested. Several experiments concerning fluid filling and encapsulation in the device have been conducted to practically study the critical issues involved therein such as the ability to fill fluid without any bubble entrapment.

Figures 15 and 16 show the schematic drawings of the MHT energy generator device. The device comprises of an energy harvesting chamber and two hydraulically amplified, piezoelectrically driven valve units. Multiple tiny PZN-PT piezo cylinders serve as energy harvesting elements in the harvesting chamber and as actuation drive elements in the active valves. Each active valve unit features multiple valve heads acting in parallel to regulate the flow through the device. The device will be assembled from 9 independent layers (4 pyrex layers and 5 silicon layers) aligned and sandwiched together using diffusion bonding between SOI wafers, anodic bonding between Si and glass interfaces and eutectic bond between Si and the piezo material interfaces.

The design of the MHT energy generator was completed in July 2000; currently, the micro-fabrication of the device and various component studies are currently underway. Assembly and testing of the MHT energy generator are expected to be completed by early summer 2001.

Continued

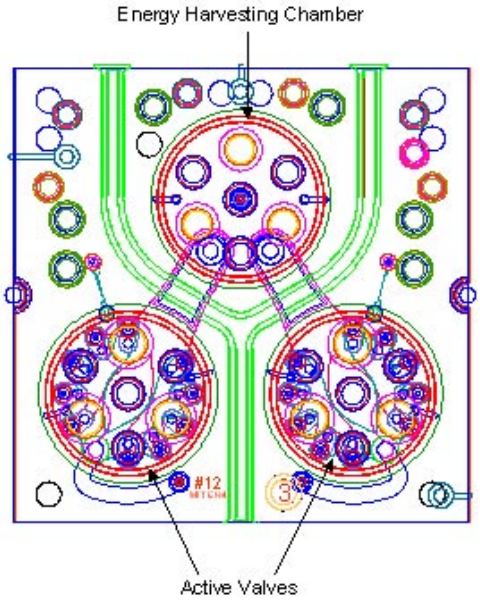

Fig. 15: Top view of the Micro-Hydraulic Energy Generator

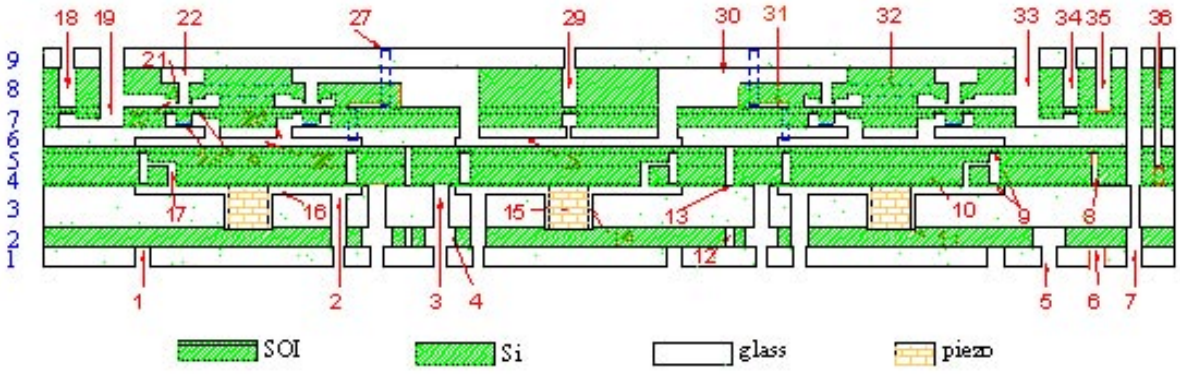

Fig. 16: Cross-sectional view of the Micro-Hydraulic Energy Generator

Vibration-To-Electric Energy Conversion

Personnel

J. O. Mur-Miranda
(J. H. Lang and A. P. Chandrakasan)

Sponsorship

Not Indicated

The goal of this project is to develop an energy scavenger that can convert ambient vibration energy into electric energy for general-purpose use. The energy scavenger employs a microelectromechanical spring-mass resonator to drive a variable capacitor which serves as the energy converter. Since the power available from ambient vibrations is generally very limited, the control, power and load electronics which drive and follow the energy converter must be designed accordingly.

To date, the microelectromechanical resonator and variable capacitor have been designed, and fabrication is underway. Additionally, very-low-power control and power electronics have been designed, fabricated and successfully tested. The design and test results indicate that, under reasonable vibration scenarios, the energy scavenger could convert approximately 20 μW of power, and deliver 50% of that power to a load. Such an energy scavenger might therefore be used to power autonomous sensors, for example.

The Polychromator: A MEMS Correlation Spectrometer

Personnel

E. Deutsch, J. Bardhan, R. Sood, and S. Vengallatore
(S. D. Senturia), in collaboration with Honeywell Technology Center and Sandia National Laboratory

Sponsorship

DARPA

There are a number of promising applications for MEMS devices in the field of optics. This project explores a particular application in infrared spectroscopy. The basic concept is to use a linear array of mirrors, each one of which can be vertically positioned throughout a gap of several microns. By adjusting the relative positions of the mirrors, it is possible to create a special kind of diffraction grating such that incident light is diffracted into a selected viewing angle at multiple wavelengths (hence the name, "Polychromator"). In particular, it is possible to create artificially the absorption or emission spectrum of a target molecule. Then, by modulating the lines in the target spectrum, one can build a new kind of correlation spectrometer — one which uses artificially created spectral features to correlate with the presence or absence of specific absorption lines in the incoming light. The Polychromator has many advantages over conventional correlation spectroscopy:

(1) the Polychromator replaces the reference gas cell with a synthetic spectral device that can be programmed for many different species;
(2) it is easy to modulate compared to gas cells;
(3) by using the emission spectrum instead of the gas-cell absorption for the correlation, the overall intensity is lowered, reducing detector shot noise; and
(4) interferences between species can be omitted from the synthetic target spectrum by design.

Device fabrication occurs as a shared Honeywell-MIT activity, and optical testing is done at Sandia Labs. MIT's contribution to this three-organization collaboration is the modeling and design of the polychromator, and electromechanical testing and voltage-displacement calibration, including material property extraction from test structures. For this latter purpose, we have developed a number of optical inspection methods. Electromechanical testing of Polychromator devices is being increasingly automated, building on the microvi-

Continued

Continued

sion system developed by Volpicelli and Sood. Bardhan has now greatly improved the robustness and capabilities of the system using correlation analysis of digitally oversampled fringe-shift patterns.

The first demonstration of gas detection by correlation spectroscopy using synthetic spectra generated by the Polychromator grating was completed this past year (see Figure 17) and reported at the Hilton Head 2000 Conference. Gas is detected in the sample cell if a modulated output signal results from switching between two spectral profiles. In order to detect carbon dioxide a spectral band-pass at the CO2 absorption at 2.350 μm-1 and a dual-band-pass with equal area outside the CO2 absorption were designed (see Figure 18). Algorithms are used to calculate the deflection profile of grating elements required to produce the spectrum and measured voltage/displacement data are used to calculate the voltages required to actuate the Polychromator. While switching between these two states, 1000 ppm CO2 is admitted to the sample cell and purged 3 times. This is detected as an increased synchronously demodulated signal when the CO2 is present as shown in Figure 19. In addition to detection of a single species this technique can be used to differentiate between several species with overlapping spectral features. Two hydrocarbons, toluene and hexane, were detected and differentiated by generating band-pass spectra that would be selective for each species and then modulating the grating between each state.

We are also studying the shock-survivability of the Polychromator in support of its eventual deployment. This is reported separately (see "Reliability of MEMS

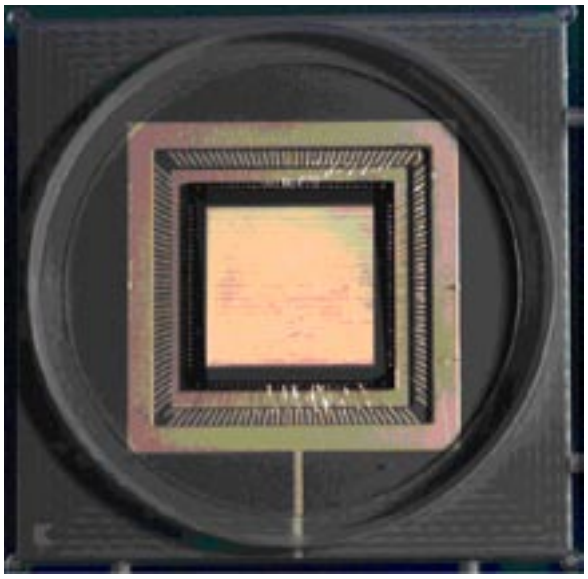

Fig. 17

Continued

Continued

Devices in Shock Environments").

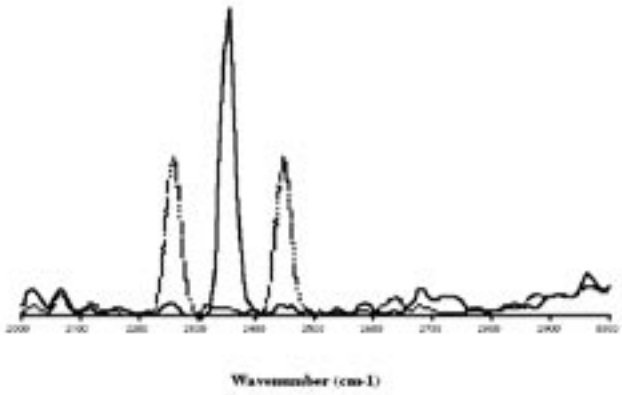

Fig. 18

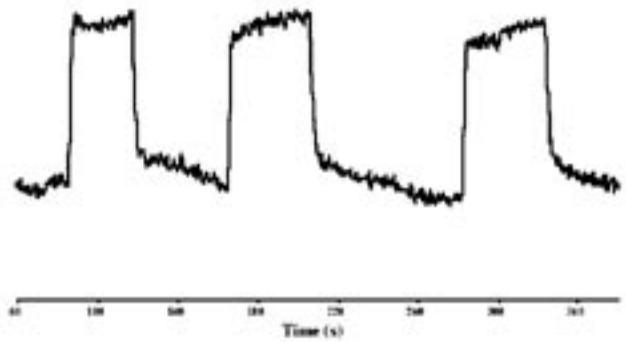

Fig. 19

Dynamical Macro-Models for Magnetic MEMS Devices

Personnel

M. Varghese-(S. D. Senturia) in collaboration with the research groups of J. K. White of MIT, J. Gilbert at Coventor (formerly Microcosm Technologies), and M. Allen of Georgia Tech

Sponsorship

DARPA and Sandia Labs

The MIT MEMCAD System has emphasized quasi-static 3-D numerical simulations of meshed structures as the basis for device modeling. However, designers typically prefer to work with dynamical analytical models with only a few degrees of freedom; we refer to these as "macro-models."

There has already been extensive work on automatic generation of macro-models for electrostatically actuated deformable elastic structures (see "CAD for Microelectromechanical Systems (MEMCAD)"). We are now extending these concepts to devices that incorporate magnetic interactions, either for sensing or actuation. In addition, we are currently fabricating magnetic MEMS test structures for verification of our reduced order models. The structures are made using a three layer process with Ni/Fe electroplated into photoresist molds. Test structures for measuring both magnetic and mechanical material properties are included in our design. Our ultimate goal is to build an electrostatically actuated flux magnetometer using this process, and model it using our reduced-order modeling methodology.

Opposite Page:

(a) Double-gate (DG) NMOS transistor with 25 nm effective channel length. Gate-to-gate alignment is via IBBI.
(b) DG-NMOS device after top-gate X-ray lithography. Alignment of gates is via IBBI.
Courtesy: A. Lochtefeld, M. Meinhold, D. A. Antoniadis and H. I. Smith.
Research sponsored by DARPA and ONR